

Christian Günz

Good practice guide to ensure complete conversion from para to normal hydrogen of vaporized liquified hydrogen

ISSN 2751-6598
ISBN 978-3-944659-24-4

DOI 10.7795/110.20221115

Physikalisch-Technische Bundesanstalt

Metrologie

PTB-M-2

Braunschweig, November 2022

Christian Günz

Good practice guide to ensure complete conversion from para to normal hydrogen of vaporized liquified hydrogen

A4.3.1: Good practice guide

ISSN 2751-6598

ISBN 978-3-944659-24-4

DOI 10.7795/110.20221115

Empfohlene Zitierweise/recommended citation

Günz, C. 2022. *Good practice guide to ensure complete conversion from para to normal hydrogen of vaporized liquified hydrogen: A4.3.1: Good practice guide.*

Braunschweig: PTB Open Access Repository.
PTB-Bericht M-2. ISBN 978-3-944659-24-4.

Verfügbar unter:

<https://doi.org/10.7795/110.20221115>

Herausgeber:

Physikalisch-Technische Bundesanstalt
ISNI: 0000 0001 2186 1887

Presse und Öffentlichkeitsarbeit

Bundesallee 100
38116 Braunschweig

Telefon: (05 31) 592-93 21

Telefax: (05 31) 592-92 92

www.ptb.de



Good practice guide to ensure complete conversion from para to normal hydrogen of vaporized liquified hydrogen

A4.3.1: Good practice guide

Author	Christian Günz
Confidentiality:	Public
Submission date:	8 th of November 2022
Revision:	1.0

methyinfra.ptb.de

Good practice guide A4.3.1	
Funding	Grant agreement no:
European Metrology Program for Innovation and Research	20IND11
Project name	Project short name
Metrology infrastructure for high-pressure gas and liquified hydrogen flows	MetHyInfra
Author(s)	Pages
Christian Günz PTB christian.guenz@ptb.de	32 pages
Summary	
<p>This report was written as part of activity 4.3.1 from the EMPIR Metrology infrastructure for high-pressure gas and liquified hydrogen flows (MetHyInfra) project. The three-year European project commenced on 1st June 2021 and focused on providing metrological infrastructure and traceability for high pressure hydrogen flow meter calibration (1000 bar / 3.6 kg/min), fuel cells applications (4 kg/h, 30 bar) and liquid hydrogen. For more details about this project please visit methyinfra.ptb.de.</p> <p>This report examines how the two spin isomers of hydrogen, namely para and ortho hydrogen, can influence the measurement of its flow which is of particular interest for vaporized liquid hydrogen. Based on differences in physical properties, flow measurement methods which are affected by the para to ortho ratio are identified. The widely used ortho para catalyst hydrous ferric oxide is introduced and its applicability for the conversion from para to equilibrium hydrogen is discussed. A practical example including the calculation of the required amount of catalyst is given. Alternative approaches to the use of a catalyst as well as measurement methods for the determination of the para to ortho ratio are provided as well.</p>	
Confidentiality	Public

This project (20IND11 MetHyInfra) has received funding from the EMPIR programme co-financed by the Participating States and from the European Union's Horizon 2020 research and innovation programme.



The EMPIR initiative is co-funded by the European Union's Horizon 2020 research and innovation programme and the EMPIR Participating States

Contents

1	Introduction	1
2	Ortho and para hydrogen	3
2.1	Equilibrium and normal hydrogen	4
2.2	Differences in physical properties	5
3	Natural Conversion	8
4	Catalytic conversion	12
4.1	First order kinetics	13
4.2	Langmuir-Hinshelwood kinetics	14
5	Hydrous Ferric Oxide	15
5.1	Reaction rate constant of HFO	16
6	Required amount of catalyst	22
7	Measurement of the ortho para ratio	25
8	Summary, recommendation and outlook	27
9	Acknowledgement	28
	References	32

1 Introduction

With growing interest in hydrogen (H_2) as an alternative energy carrier, accurate methods to quantify the amount of transferred H_2 are required. Here, it is the duty of metrology and national metrology institutes to ensure the development, traceability and calibration of appropriate flow measuring devices. Especially in the case of hydrogen, this is accompanied by effects which are different to for instance natural gas or other fuels. First, liquid H_2 is stored at a very low temperature of 20 K which in itself is a challenge for any kind of flow measuring device. To ensure traceability or verify that instruments calibrated at ambient temperatures can be used, a vaporization test rig schematically illustrated in figure 1 could be utilized. The flow of liquid equilibrium hydrogen would be measured with the flow sensor under investigation. Then, the hydrogen is vaporized and the resulting gas flow is measured with the calibration instrument at around ambient conditions.

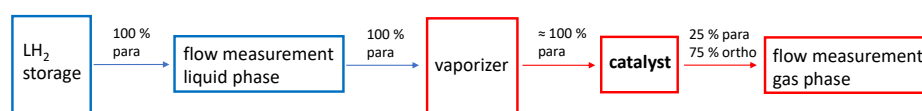


Figure 1: Schematic principle of a vaporization rig for the calibration of liquid hydrogen flow sensors.

A second challenge is a consequence of quantum mechanics which causes molecular hydrogen to consist of two different allotropes, namely ortho and para hydrogen, which are introduced in section 2. It will be shown in 2.2 that they differ significantly in certain physical properties. Three well established measuring methods will be discussed to illustrate exemplarily that these differences can lead to deviations in the order of several percent for the measurement of hydrogen flow. Additionally, the equilibrium concentrations of the allotropes are strongly temperature dependent. While at low temperatures para hydrogen is present almost exclusively, the ratio changes to 25 % para and 75 % ortho hydrogen (so called normal hydrogen) at ambient temperatures. The natural conversion between para and ortho hydrogen is a forbidden transition and, thus, a comparably slow process that will be shortly summarized in section 3. It can, therefore,

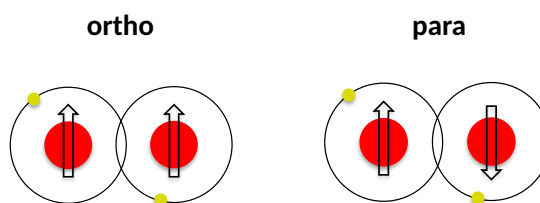
not be assumed that hydrogen will be in equilibrium composition after changes of temperatures. Theoretically, the hydrogen composition could be measured together with the flow. Appropriate techniques will be shown in section 7 by the end of this guide. However, a more sophisticated approach is to ensure that the hydrogen is in equilibrium. Especially in the field of hydrogen liquefaction, catalysts are already established to reach this goal. They could be utilized here as well and would have to be incorporated prior to the gas flow measurement as shown in figure 1. A general introduction to the catalytic conversion of hydrogen will be given in section 4. Currently, the by far most used catalyst for ortho para conversion is the commercially available hydrous ferric oxide (HFO). Therefore, it will be discussed in this study as well. Its properties and particularly the volumetric reaction rate constant for the para to ortho conversion are summarized in section 5. Based on this information, recommendations and an example calculation will be given in section 6 to solve the key question: How to estimate the required amount of catalyst to ensure complete conversion from para to normal hydrogen for a certain mass flow. Two remarks have to be made at this point. First, there is a rather promising alternative approach which does not require the utilization of a catalyst. If the initial composition is known, for instance because liquid equilibrium hydrogen (99.8 % para hydrogen) is vaporized, it can be assumed that the gas has the same composition as long as it is not exposed to catalytically active materials and as long as the time scales are short. Corresponding estimations of these times can be performed based on the information on the natural conversion in section 3. However, this approach is not extensively discussed in this guide. The second remark is that several but not all flow measuring methods are influenced by the para ortho hydrogen ratio. Examples of unaffected methods will be given in the summary 8 by the end of this guide.

This guide was written based on a literature study and experiences gained for the process of hydrogen liquefaction. Experienced actors from industry and academics were contacted to provide the best strategy. A possible enhancement of the para ortho conversion rate based on the application of an external magnetic field as reported by several authors [1–5] is not part of this study.

Disclaimer: Commercial products, hard- and software identified throughout this guide does not imply recommendation or endorsement by Physikalisch-Technische Bundesanstalt (PTB), nor does it imply that identified equipment is the best for this purpose.

2 Ortho and para hydrogen

The existence of ortho and para hydrogen was already postulated in 1927 as a consequence of quantum mechanical considerations, whereas the experimental verification followed two years later [6]. The allotropes differ in the orientation of the nuclear spins of the two hydrogen atoms forming the molecule. A short, direct comparison is given in table 1.



	ortho	para
nuclear spin orientation	parallel	anti parallel
nuclear spin quantum number I	$1 \left(\frac{1}{2} + \frac{1}{2} \right)$	$0 \left(\frac{1}{2} - \frac{1}{2} \right)$
rotational quantum number J	odd $J = 2n - 1$	even $J = 2(n - 1)$
lowest state	$J = 1$ (triplet state)	$J = 0$ (singlet state)
magnetic moment	yes	no

Table 1: Comparison of ortho and para hydrogen. $n \in \mathbb{N}$

According to the Pauli principle, the wave function of the hydrogen molecule has to be anti-symmetrical. The overall wave function is the product of the wave functions of vibration, rotation and spin. The wave function of vibration is the same for both allotropes. However, since the nuclear spin is symmetric for ortho and anti-symmetric for para hydrogen, the opposite has to be true for the rotational wave functions. They are anti-symmetric (odd quantum numbers) for ortho and symmetric (even quantum number) for para hydrogen. A consequence is that para hydrogen exhibits the lowest possible energy state for the nuclear spin quantum number $I = 0$ and the rotational quantum number $J = 0$. This singlet state has no rotational component. The next energy level corresponds to the ortho modification with $I = 1$ and $J = 1$ which is a triplet state.

2.1 Equilibrium and normal hydrogen

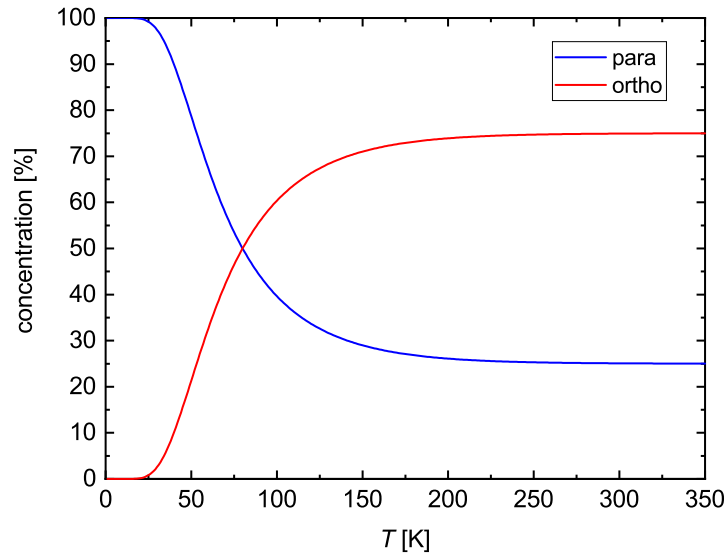


Figure 2: Equilibrium concentrations of ortho and para hydrogen as a function of temperature T calculated by equation 1.

A consequence of the previous section is that four different states are likely to be populated depending on the temperature T . The corresponding probabilities are defined by the Boltzmann distribution whereas the ratio between the mole fractions χ of para and ortho hydrogen can be approximated by [7, 8]:

$$\frac{\chi_{\text{para}}}{\chi_{\text{ortho}}} \approx \frac{1}{3} \cdot \frac{1 + 5 \exp \frac{-6B}{k_B T} + 9 \exp \frac{-20B}{k_B T} + 13 \exp \frac{-42B}{k_B T}}{3 \exp \frac{-2B}{k_B T} + 7 \exp \frac{-12B}{k_B T} + 11 \exp \frac{-30B}{k_B T}} \quad (1)$$

In this formula k_B is the Boltzmann constant and B is the rotational constant of the H_2 molecule which is defined and calculated by:

$$B = \frac{h^2}{8\pi^2 I_{\text{H}_2}} = 1.209 \cdot 10^{-21} \text{ J} \quad (2)$$

h is the Planck constant and $I_{\text{H}_2} = 4.5992 \cdot 10^{-48} \text{ kgm}^2$ is the moment of inertia of the hydrogen molecule [8]. In figure 2, the resulting composition of the equi-

librium hydrogen as a function of temperature is plotted. For low temperatures, the energetically favorable para configuration is populated almost exclusively (approximately 99.8 % para 0.2 % at 20 K). With rising temperatures the amount of the ortho configuration increases. At temperatures above 250 K the concentration ratio is approximately 75 % ortho and 25 % para hydrogen displaying the ratio between triplet and singlet states. Hydrogen with this composition (regardless of temperature) is referred to as normal hydrogen.

2.2 Differences in physical properties

As already stated in the introduction, para and ortho hydrogen differ significantly in certain physical properties. The most prominent example is the thermal conductivity λ . Relative differences between para and normal H₂ gas were calculated for a pressure of 0.1 MPa using the most recent correlation by Assael *et al.* [9]. The values are plotted in figure 3. Deviations exceed more than 25 % at temperatures around 150 K and are still in the order of almost 5 % around ambient conditions. Among the caloric properties, the heat capacities are also significantly different. Absolute, specific values of c_p are plotted in figure 3 b). As a consequence, the speed of sound u , which is proportional to the square root of the adiabatic index, is also different for para and ortho and, thus, normal hydrogen. The relative difference between the speed of sound u for para and normal H₂ is plotted as a function of temperature in figure 3 c). At about 120 K the maximum difference of about 5.5 % occurs whereas it is still in the order of one percent around room temperature. The values for c_p and u were generated using the reference equation of state (EOS) for hydrogen by Leachman *et al.* [10].

These differences in physical properties impact certain flow measurement methods. Three examples are depicted in figure 4. In a) a thermal flow meter is shown. It incorporates two Pt100 temperature sensors which are positioned inside the gas stream. While one of them measures the actual temperature of the gas, the other one is electrically heated. The flowing gas will draw heat from the heated sensor whereas the heat loss depends on the flow. Two modes of operation are possible. Either the heating current is adjusted to maintain a constant temperature difference between both sensors ("rate of loss flow meter") or the heating current remains constant and the change in temperature difference between both

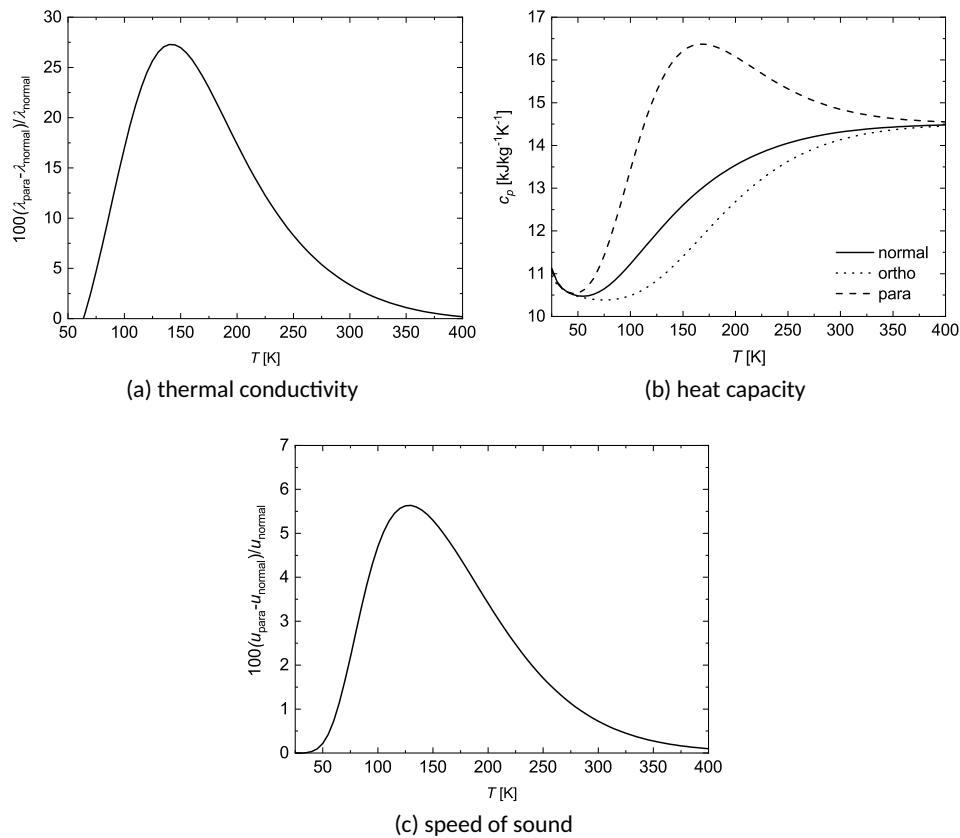


Figure 3: Differences in certain physical properties at a pressure of 0.1 MPa as a function of temperature. a) Relative difference between the thermal conductivity for para and normal hydrogen in percent. The values were calculated by the correlation of Assael *et al.* [9] b) Absolute values for the specific isobaric heat capacities for para-, ortho- and normal hydrogen. c) Relative deviation between the speed of sound u of para and normal hydrogen in percent. Plots b) and c) were prepared utilizing the EOS of Leachman *et al.* [10]

sensors is measured (“temperature rise thermal flow meter”). The gas flow can be calculated if among other parameters the thermal conductivity and heat capacity are known. The differences of these caloric properties for ortho and para hydrogen depicted in figure 3 a) and b) will, thus, directly change the displayed flow. A second example is ultrasonic flow meters shown in 4 b). Typically, these instruments have two transducers to measure the speed of sound up- and downstream. This way the actual speed of sound in the medium can be excluded from the working equation. However, modern sensors also compare the directly measured speed of sound to one which is determined from additional internal temperature and pres-

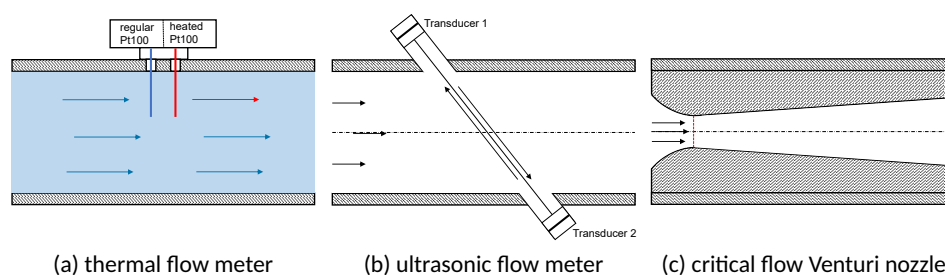


Figure 4: Examples of three different flow measuring methods that are affected by the ortho para ratio. The working principles are explained in the text.

sure measurements and a corresponding EOS. If the ortho para ratio is not taken into account properly, the differences in the speed of sound shown in figure 3 c) may cause error messages. A final example is the widely used critical flow Venturi nozzle (see figure 4 c)). Here, the flow is choked if the velocity of the medium reaches the local speed of sound at the point with the smallest diameter of the nozzle, which is indicated by the red line. In choked conditions, changes of pressure downstream of the nozzle will not change the flow. However, differences in the speed of sound caused by changes of the ortho para ratio also directly change the mass flow. It can be seen from figure 3 c) that deviations of several percent are possible.

Beyond the three examples, minor differences can be observed for the density of para and ortho hydrogen gas by using the EOS by Leachman *et al.* These deviations are far below the uncertainty in density of 0.04 % valid for the temperature range from 250 K up to 450 K and can, thus, be neglected. However, it should also be pointed out that the vast majority of the underlying data for the EOS were already measured in the 60s or even earlier. That is why, besides this guide, efforts to measure the speed of sound and density virial coefficients of hydrogen are also part of the EMPIR-project MethHyInfra which will be acknowledged at the end of this document. Furthermore, very small differences in the viscosity were reported by Mehl *et al.* for low temperatures but will not be further discussed here [11].

3 Natural Conversion

It was shown in figure 2 that the composition of hydrogen changes with temperature. This plays a major role for the liquefaction of gaseous H₂ (see, for instance, the recent review on hydrogen liquefaction by Al Ghafri *et al.* [12]). When the gas is cooled down, ortho hydrogen has to be converted to para hydrogen whereas the natural conversion is slow since this is a forbidden transition. The reaction itself is exothermic since the rotational energy of the ortho hydrogen is converted to heat. Since the heat of conversion is larger than the heat of vaporization, a significant amount of the liquid is re-vaporized if the ortho hydrogen is not converted to para prior to the liquefaction. After 100 hours, 40 % of the liquified hydrogen is evaporated again [6, 13]. A detailed plot of the expected boil off as a function of time and initial ortho concentration is shown in figure 56 of the very comprehensive NBS Monograph 168 on selected properties of hydrogen [14]. A detailed study of the heat of conversion is given in reference [15].

The natural conversion from para to ortho hydrogen was investigated by several authors for the solid, liquid and gas phase. It was already shown in 1929 that ortho H₂ has a magnetic moment causing it to act as a catalyst itself [16]. Since the ortho hydrogen concentration and, thus, the amount of catalyst changes over the course of the conversion, the process is a second order process, whose kinetics are described by [17, 18]:

$$-\frac{d\chi_{\text{ortho}}}{dt} = k\chi_{\text{ortho}}^2 - k'\chi_{\text{ortho}}(1 - \chi_{\text{ortho}}) \quad (3)$$

k and k' are the reaction rate constants for ortho to para conversion (k - forward reaction) and para to ortho conversion (k' - reverse reaction) respectively. They are pressure and temperature dependent. χ_{ortho} is the fraction of ortho hydrogen and $\frac{d\chi_{\text{ortho}}}{dt}$ denotes the change of ortho concentration over time. It should be pointed out that since k and k' are both included, equation 3 and the equations derived from it in the following describe not only the forward but also the reverse reaction.

Since ortho hydrogen is only converted to the para configuration, it is true that $\frac{d\chi_{\text{ortho}}}{dt} = -\frac{d\chi_{\text{para}}}{dt}$. Furthermore, the two reaction rate constants can be brought into relationship by investigation of equilibrium conditions where $\frac{d\chi_{\text{ortho}}}{dt} = 0$:

$$K = \frac{k'}{k} = \frac{\chi_{\text{ortho,e}}}{1 - \chi_{\text{ortho,e}}} \quad (4)$$

The ratio K can, thus, be determined from the equilibrium concentration $\chi_{\text{ortho,e}}$. Replacing k' in equation 3 and integration results in:

$$-\int_{\chi_{\text{ortho,in}}}^{\chi_{\text{ortho,out}}} \frac{1}{\chi_{\text{ortho}}^2 + K\chi_{\text{ortho}} - K} d\chi_{\text{ortho}} = k \int_0^{\tau} dt \quad (5)$$

In this case τ is the average time the hydrogen has contact with a catalyst. The integration yields the following result:

$$k = -\frac{1}{\tau K} \ln \left(\frac{|(\chi_{\text{ortho,out}} - \chi_{\text{ortho,e}}) \chi_{\text{ortho,in}}|}{|(\chi_{\text{ortho,in}} - \chi_{\text{ortho,e}}) \chi_{\text{ortho,out}}|} \right) \quad (6)$$

Unfortunately, no data on the natural conversion rate constants was found in the literature for a temperature of 300 K. The latest experimental study covering a reasonable temperature range in the gas phase was published by Milenko *et al.* in 1997 [18]. They covered temperatures from 40 K to 120 K and pressures between 2 MPa and 70 MPa. They proposed to describe the retrieved reaction rate constants k by the following polynomial:

$$k = A_0 T^n \rho + (C_0 + DT^{-m}) \rho^{3.6} \quad (7)$$

k is given in units of 10^{-3}h^{-1} if the numeric values of temperature T and density ρ are inserted in units of K and g cm^{-3} . Deviations to their experimentally determined values are less than 4.8% for the entire range of temperatures and

pressures they covered. The corresponding parameters of equation 7 are listed in table 2.

$$\begin{aligned}
 A_0 &= (18.2 \pm 1.6) \frac{\text{cm}^3}{\text{kg} \cdot \text{h} \cdot \text{K}^n} & n &= 0.56 \pm 0.02 \\
 C_0 &= (38.5 \pm 1.5) \frac{\text{cm}^{3 \cdot 3.6}}{\text{h} \cdot \text{g}^{3.6}} & m &= 2.5 \pm 0.2 \\
 D &= (4.605 \pm 0.455) \frac{10^4 \cdot \text{K}^m \cdot \text{cm}^{3 \cdot 3.6}}{\text{h} \cdot \text{g}}
 \end{aligned}$$

Table 2: Parameters of equation 7 reported by Milenko *et al.* valid for $40 \text{ K} \leq T \leq 120 \text{ K}$ [18]. They also provided uncertainties which are fit uncertainties from the interpolation of their measurement results.

Due to the lack of data for hydrogen conversion at the temperature and pressure conditions regarded in this study, this polynomial is extrapolated to estimate reaction rate constants at 300 K. Petipas *et al.* have shown that overall the validity of the data by Milenko *et al.* increases with higher temperatures and densities [19]. An uncertainty estimate for the extrapolated values of k can be made based on the uncertainties provided by Milenko *et al.* for the parameters in table 2. For example, k has a value of $4.44 \times 10^{-4} \text{ h}^{-1}$ with a relative uncertainty of 14.4 % at 300 K and a density of 0.001 g cm^{-3} . To illustrate the principle behavior, several parameter variation plots are shown in figure 5. Plotted is always the development of the ortho hydrogen fraction over time in days. The basic assumption is that liquid hydrogen is vaporized at a temperature of 300 K unless the temperature is varied. Due to the catalytic effect of ortho hydrogen, it can be seen from (a) that the time required to reach the equilibrium concentration of 75 % is highly dependent on the overall density. A higher density increases the probability of interaction with other hydrogen molecules which reduces the time required for complete conversion. Also, since the conversion is a second order reaction, variations in the inlet ortho hydrogen concentration $x_{o,\text{in}}$ influence the conversion time. Obviously higher starting ortho concentrations result in faster conversion as shown in (b). Finally, the influence of the temperature is plotted in (c) and (d) for two different cases. In (c) the density is kept constant while the temperature is varied. This leads to the impression that higher temperatures favor a faster conversion. However, a more realistic scenario for a gas flow measurement is that the pressure remains constant. This case is shown in (d). As a consequence the particle density is decreased which results in a slower conversion.

Though some of the parameters influencing the natural conversion can be varied,

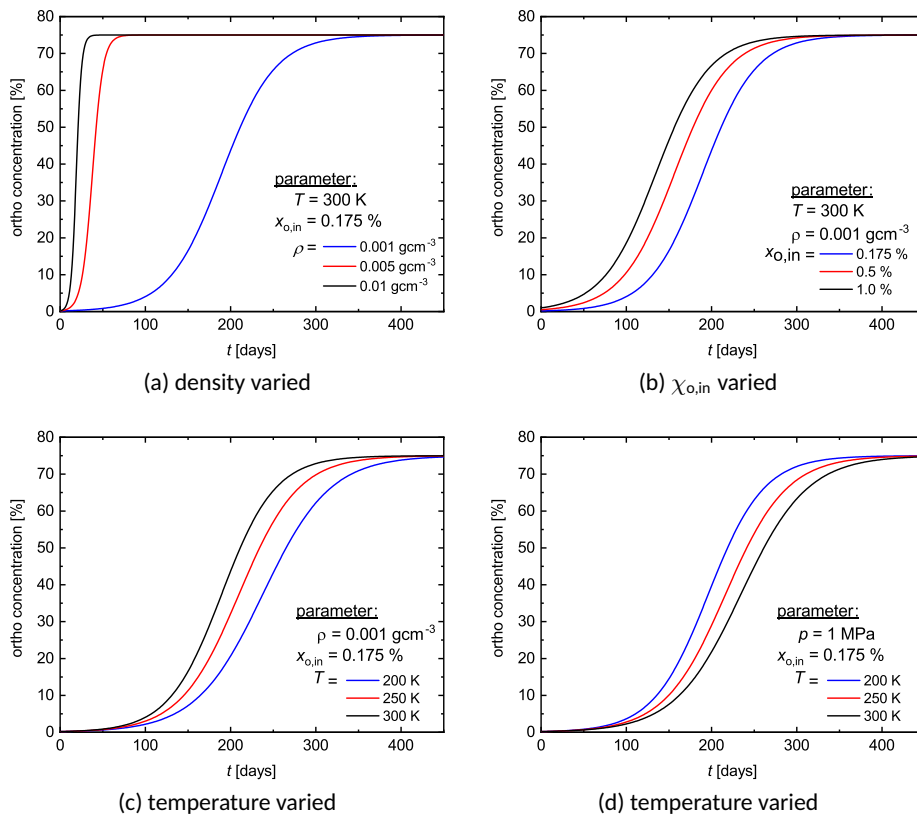


Figure 5: Conversion from para to ortho hydrogen as a function of time for different parameters calculated by combining equations 6 and 4. Plotted is always the concentration of ortho hydrogen in percent over time in days. The underlying time constants k were calculated by extrapolation of equation 7 taken from reference [18] to higher temperatures.

it is obvious that the required time for a sufficient conversion to normal hydrogen is still within the order of days or weeks. These time scales are confirmed by thorough studies of Petipas *et al.* and Matthews *et al.* [19, 20]. Petipas *et al.* investigated the time until overpressure causes hydrogen venting from a full-scale cryogenic storage vessel for automotive applications. The slow natural conversion can be exploited to derive an alternative approach besides the utilization of a catalyst. As long as the time scales are short and the contact time to catalytic materials is sufficiently minimized, it may be assumed that the vaporized hydrogen gas remains in close to 100 % para configuration. For large flow rates these conditions can probably be met. However, it has to be taken into account that ferromagnetic surfaces and in particular steel act catalytic as well. That is why it is advisable in

most cases to determine the actual para to ortho ratio. An overview of applicable measurement methods will be given in section 7.

4 Catalytic conversion

The slow natural conversion leading to the aforementioned difficulties for the liquefaction of hydrogen caused major interest in the catalytic conversion within the frame of the space programs in the 50s and 60s where large amounts of liquid hydrogen were required as a propellant for rockets. While it was for instance already shown in 1933 by Farkas and Sachse that oxygen acts as a catalyst [21, 22] in this regard, obviously only a heterogenic catalytic reaction using a solid catalyst can be used for this purpose. Several materials were investigated for their catalytic potential for the space programs in the US and the former Soviet Union as well as for the realization of the hydrogen triple point which is a fix point in the International Temperature Scale of 1990 [23, 24]. A profound overview of the different catalysts and possible conversion mechanisms is for instance given by Ilisca [25] or Al Ghafri *et al.* [12]. The overall process consists of seven steps independent from the specific catalyst [6]:

1. diffusion from the main gas stream to the surface of the catalyst
2. diffusion into the pores of the catalyst
3. adsorption on the catalyst
4. reaction (conversion) by interaction with the magnetic centers
5. desorption from the catalyst
6. diffusion out of the pores of the catalyst
7. diffusion from the catalyst to the main gas stream

The conversion is obtained by an interaction between the magnetic centers of the catalyst and the H₂ molecule whereas the spin flip typically occurs without dissociation of the molecule. Exceptions where hydrogen is dissociated exist for certain

catalysts [6]. While the conversion only takes place in step 4, each one of the steps could be the slowest, thus, rate determining step. It was shown that the diffusion from and back to the main gas stream (steps 1 and 7) is rather unlikely to be limiting in this regard [6]. The effect of pore diffusion (steps 2 and 6) can be neglected if the grain size is reduced below a certain level which will be shortly discussed in section 5.1 [6, 26]. In case that step 4, the actual conversion, is rate determining, a simple first order approach is sufficient to describe the kinetics. If adsorption and desorption play a role as well, Langmuir-Hinshelwood kinetics can be applied. Both cases will be briefly introduced in the following. Further aspects that influence the conversion will be shortly summarized in subsection 5.1.

4.1 First order kinetics

The first order reaction approach was used by several authors particularly in the earlier phase of research in this field (see for instance publications by Weitzel *et al.* from the 1950s [26–28], the publication summarizing the effort in the former Soviet Union by Zhuzhgov *et al.* [23], or also references [17, 29, 30] and references within them). The corresponding rate equation is [17]:

$$-\frac{d\chi_{\text{ortho}}}{dt} = k\chi_{\text{ortho}} - k'(1 - \chi_{\text{ortho}}) \quad (8)$$

The investigation of the equilibrium conditions for $\frac{d\chi_{\text{ortho}}}{dt} = 0$ yields the same result for the ratio of both reaction constants as equation 4. Combination with equation 8 leads to the integral:

$$-\int_{\chi_{\text{ortho,in}}}^{\chi_{\text{ortho,out}}} \frac{1}{\chi_{\text{ortho}} + K\chi_{\text{ortho}} - K} d\chi_{\text{ortho}} = k \int_0^{\tau} dt \quad (9)$$

Integration yields the following relation:

$$k = -\frac{1}{\tau (K + 1)} \ln \left(\frac{|\chi_{\text{ortho,out}} - \chi_{\text{ortho,e}}|}{|\chi_{\text{ortho,in}} - \chi_{\text{ortho,e}}|} \right) \quad (10)$$

Though equation 10 allows to retrieve the reaction constant k from experimental data, the contact time to the catalyst τ is hard to determine. That is why experiments are typically realized by flowing gas through an in-line packed bed catalytic reactor. A simpler formulation beneficial for these flow experiments is [23]:

$$k_V = \frac{n}{t} \frac{1}{V_{\text{cat}}} \ln \frac{1 - \frac{\chi_{\text{para,in}}}{\chi_{\text{para,e}}}}{1 - \frac{\chi_{\text{para,out}}}{\chi_{\text{para,e}}}} \quad (11)$$

In this equation, the para H₂ concentrations are used which will be beneficial later. $\frac{n}{t}$ is the molar flow in mol s⁻¹ and V_{cat} is the volume of the catalyst in cm³. The volumetric reaction rate constant of the catalyst k_V therefore has the unit mol cm⁻³ s⁻¹ and does relate to the overall conversion velocity. It is not differed between forward and reverse reaction.

4.2 Langmuir-Hinshelwood kinetics

Deviations to the previously introduced linear behavior became apparent in the 60s [6, 26, 29–33]. As consequence, also Langmuir-Hinshelwood kinetics which additionally includes adsorption and desorption (steps 3 and 5) was applied. Hutchinson investigated both mechanisms as well as two more approaches in his PhD thesis [30, 32]. Recently, Donaubaue *et al.* published a corresponding rate equation for the ortho to para conversion based on data sets published in the 60s [34]. However, the corresponding rate equation and formulas are not introduced and discussed here in detail since it will be shown in section 5.1 that the few available data sets used in this study can be sufficiently described by the simpler 1st order approach.

5 Hydrrous Ferric Oxide

As already mentioned previously, a large number of catalysts was investigated throughout the last decades whereas the main field of application is still hydrogen liquefaction. The author of this guide surveyed the largest producers in this field as well as academic institutes related to this field and it was revealed that Hydrrous Ferric Oxide (HFO) is practically used exclusively at this point. It is distributed under the name IONEX[®] Type O-P by Molecular Products Inc. [35] whereas the chemical formula is $\text{Fe}_2\text{O}_3 \cdot n\text{H}_2\text{O}$. The particles have a size of 30 x 50 standard mesh size (US Sieve) which corresponds to a grain size between 0.3 mm and 0.6 mm. The resulting apparent mass density of the powder is 1.20 g cm^{-3} to 1.37 g cm^{-3} . In figure 6, two microscopic images of the particles with 25 times (a) and 500 times (b) magnification are shown.

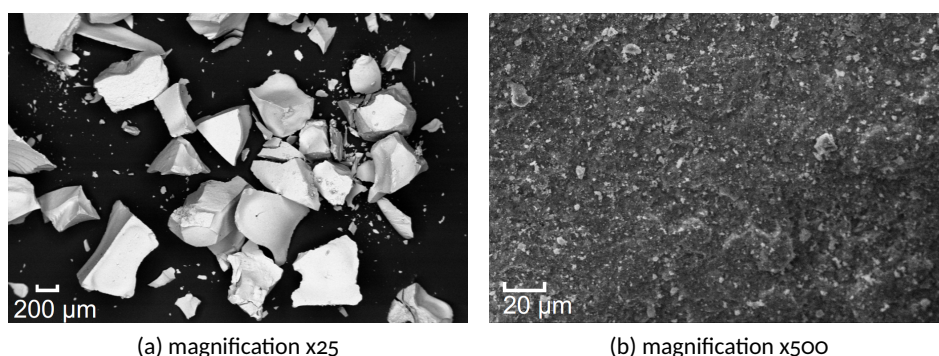


Figure 6: Microscopic images of HFO taken with kind permission from the PhD thesis of Jürgen Essler [17].

Before the delivered catalyst can be used, remaining impurities, especially water, have to be removed from the catalytic surface in an activation process. According to the supplier, the activation shall be performed by heating the catalyst to 160°C while establishing a dry hydrogen flow for 16 hours. The disadvantage of this procedure is the relatively high consumption of hydrogen as well as the comparably high temperature. That is why Essler and Haberstroh published a detailed study where the activation of the IONEX[®] type O-P catalyst was investigated [36]. They were able to show that the performance of the catalyst can be maintained even if the activation temperature is lowered to 120°C . In his PhD thesis, Essler also showed that instead of hydrogen gas much cheaper nitrogen gas can be used for activation [17].

5.1 Reaction rate constant of HFO

To estimate the required amount of HFO for complete conversion from para to equilibrium (or normal) hydrogen at a given temperature, pressure and flow, the volumetric reaction rate constant k_V defined in equation 11 is required. Most of the available literature values of this property were determined with regard to applications in hydrogen liquefaction and, thus, for cryogenic temperatures of 90 K and below. Around ambient temperature no data are available. That is why an extensive literature study was undertaken to investigate the temperature dependence of k_V and extrapolate up to 300 K. For this purpose, well documented data sets that show an incomplete conversion from para to ortho hydrogen are required. From these, k_V can be calculated by the formulas introduced in section 4.1.

In principal, data obtained for the forward reaction (ortho to para conversion) could also be used. The formulas introduced in subsection 4.1 indicate that the forward and reverse reactions always happen simultaneously. Furthermore, a substantial amount of data is available for the forward reaction with HFO since this is the one required for liquefaction and, thus, the main application. Current publications in this field which cite a lot of the older work (for instance references [26, 28]) were written by Donaubauer *et al.* and Zhuzhgov *et al.* [23, 34]. The first determined the coefficients for a Langmuir-Hinshelwood rate equation for the temperature range between 20 K and 90 K while the latter summarized the efforts of the space program in the former Soviet Union relying on a 1st order reaction. Unfortunately, Hutchinson showed in his PhD thesis [30] and two following articles [32, 33] that the reaction kinetics are not fully understood. He tested four different equations corresponding to different kinetics including the already introduced linear approach (see 4.1) and Langmuir-Hinshelwood kinetics (see 4.2). Most of them can be used to describe the reactions in forward or reverse direction but only one of them, a quite complex logarithmic approach, seemed to be suitable to describe the overall reaction (forward and reverse combined). However, Hutchinson could only test this particular approach for one temperature of 76 K. In 2018, Wilhelmsen *et al.* determined the parameters of this logarithmic approach based on available experimental data for HFO in a wider temperature range from 23.4 K to 85.6 K [37]. It was shown that the forward reaction can be described quite well with the derived parameters. For the reverse reaction, it can be seen from figure 6 of the work by Wilhelmsen *et al.* that the deviations between experimental

data points and the derived logarithmic approach are in the order of 5 % for the para hydrogen concentration. That is why the author of this guide refuses to use the logarithmic approach for extrapolation to higher temperatures. Since none of the reaction kinetics properly describes forward and reverse reaction, the reaction mechanism itself is not fully understood at this point due to the principle of microscopic reversibility and should be topic of further research. An effect that may play a role in this regard is the favored adsorption of ortho hydrogen in comparison to para hydrogen [30, 34, 38]. A direct consequence is, that the data available for the forward reaction cannot be used to extract values for the reverse reaction.

That is why, only the data directly obtained for the para to ortho conversion can be utilized. Furthermore, the temperature dependence itself should be studied to some extent. Otherwise the variety of parameters that can influence the volumetric reaction rate constant will severely complicate the comparison and extrapolation of data from different publications. A list of these influencing parameters is given by the end of this section. Unfortunately, only two data sets in the literature were found which fulfilled the stated conditions. One data set that was obtained within the master thesis of Hutchinson and then published in a separate article covers a temperature range from 40 K to 80 K and a broad pressure range from 0.29 MPa up to 7.0 MPa [29, 31]. The original plot which is included in both references is shown in figure 7 (a). For this study, the data set with a low pressure of 0.29 MPa was selected since it is most similar to the pressure of the second data set which will be introduced next. Shown is the para hydrogen content in percent as a function of space velocity SV which is defined as the volumetric gas flow at a certain temperature and pressure divided by the volume of the catalyst. The resulting unit is inverse time (in this case “per minute”). Hutchinson selected the temperature and the pressure inside the catalytic cell as reference (SV_{cat}). In other publications, typically, the space velocity SV_{STP} at standard conditions is used. Hutchinson calculated $SV_{\text{cat}} = SV_{\text{STP}} \frac{\rho_{\text{STP}}}{\rho_{\text{cat}}}$ to convert to the pressure and temperature conditions at the catalyst. ρ_{STP} and ρ_{cat} denote the mass densities of the hydrogen gas at STP conditions and the temperature and pressure at the catalyst, respectively. For the higher temperature range, only one publication with a useful data set was found. Weitzel *et al.* published a very thorough study on hydrous ferric oxide as Technical Memorandum No. 55 in NBS report 5515 (NBS project 8120-12-8629) in 1957 [27]. It shall not be confused with a contribution in *Advances in Cryogenic Engineering* that has the same title [28]. The study and the

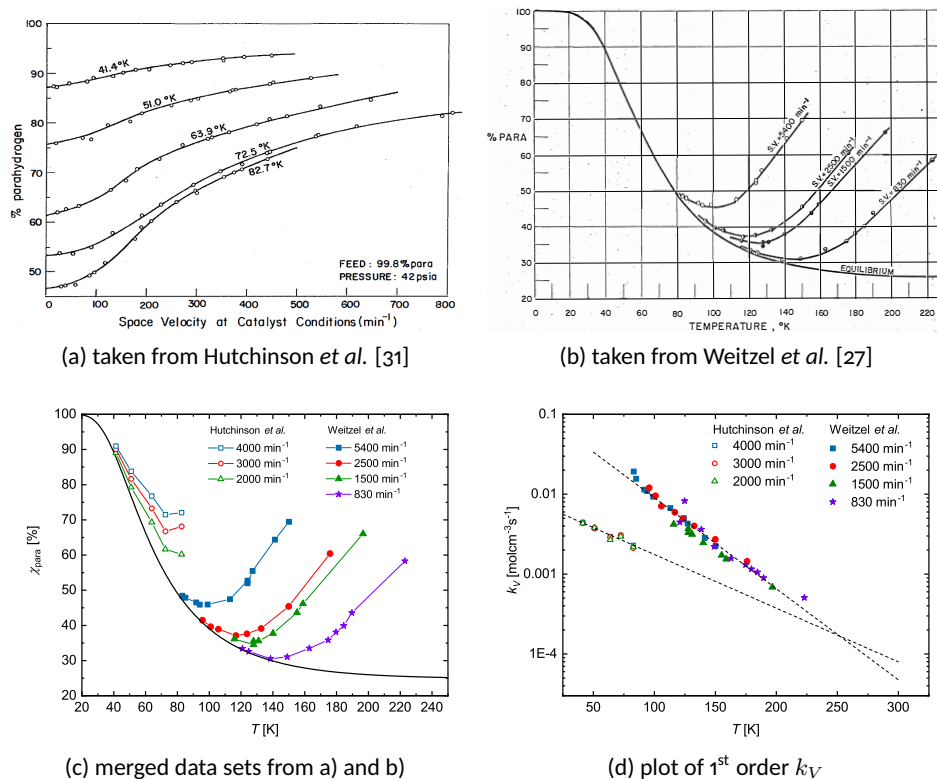


Figure 7: Plots from the original publications by a) Hutchinson *et al.* for 0.29 MPa [31] and b) Weitzel *et al.* for 0.2 MPa [27]. In both cases the initial para concentration was 99.8%. Plotted is the remaining concentration of para hydrogen in percent over the space velocity at the pressure and temperature conditions of the catalyst for different temperatures in a). In b) the para concentration is plotted over the temperature of the catalyst for several space velocities at STP conditions (standard temperature and pressure), respectively. c) Shows the merged data sets from a) and b) by means of the para hydrogen concentration in percent plotted over temperature. Details on the conversion from space velocity at catalyst conditions in plot a) to space velocity at STP conditions used in plot b) is given in the text. d) The volumetric reaction rate constants calculated by equation 11 from the data points shown in c) assuming a 1st order reaction are plotted over temperature including linear fits (dashed black lines)

NBS report is focused on the ortho to para direction but, in the very end, one plot (number 9) shows data for incomplete conversion from para to ortho hydrogen at a pressure of 0.2 MPa. It is depicted in figure 7 (b). Plotted is the remaining para hydrogen content after feeding a catalytic converter with 99.8% para hydrogen at the inlet as a function of temperature and a pressure of 15 psig corresponding to

a gauge pressure of 0.1 MPa. The equilibrium concentration is plotted as a reference as well. Here, the space velocity at STP conditions (in 1957: 273.15 K and 101.325 kPa) is used. For rising temperatures, the remaining para concentrations increase which corresponds to a less complete conversion.

To merge both data sets, the measuring points by Weitzel *et al.* were digitized and the ones from Hutchinson were converted to the STP conditions used by Weitzel *et al.* Since the density tabulations Hutchinson used to calculate SV_{cat} are not available, the required values were calculated based on equations for SV_{STP} provided in appendix I in combination with data for the individual measuring runs provided in appendix J of the master thesis of Hutchinson [29]. Then, for figure 7 (a), the intercepts between vertical lines of constant space velocity and the para hydrogen content at constant temperatures were used to generate data sets in analogy to figure 7 (b).

The combined data sets are shown in figure 7 (c). The qualitative trend is similar for the two data sets, with both featuring a minimum in χ_{para} . However, a direct comparison at 80 K reveals discrepancies for similar space velocities of 4000 min^{-1} (open blue squares) and 5400 min^{-1} (solid blue squares). The deviation expressed in χ_{para} is in the order of 25 %. Possible explanations for these deviations will be given by the end of this section when a more comprehensive overall picture is obtained. In a first approach, the data points were evaluated by a 1st order reaction. Values for the volumetric rate reaction constant k_V were calculated by equation 11 and are plotted in figure 7 (d) on a logarithmic scale over temperature. Obviously, both data sets result in clearly distinct values. Though there is scatter, both data sets also show a clear linear trend (indicated by the dashed lines in figure 7 d)) with slightly different slopes. The scatter is on the one hand a consequence of the different space velocities. On the other hand a minor contribution to scatter originates from the digitization of the data points from the original plots. The linear behavior is taken as indication that the 1st order reaction describes these limited data sets sufficiently for the purpose of extrapolation. Therefore, the more complex Langmuir-Hinshelwood kinetics function (see subsection 4.2) is not applied here. A function describing the temperature dependence of k_V was fitted to both data sets and is given by:

$$k_V = a \cdot e^{-b \cdot T} \quad (12)$$

The corresponding fit parameters and uncertainties are listed in table 3.

data set	a [mol cm ⁻³ s ⁻¹]	b [K ⁻¹]
Weitzel <i>et al.</i>	0.1249 ± 0.0159	0.0263 ± 0.0009
Hutchinson	0.0083 ± 0.0007	0.0155 ± 0.0013

Table 3: Fit coefficients and fit uncertainties of the parameters of equation 12 which is used to describe the temperature dependence of k_V for the data sets by Weitzel *et al.* and Hutchinson shown in figure 7 (d).

To at least partially resolve the occurring discrepancies between the data by Hutchinson *et al.* and Weitzel *et al.* in figure 7 (c) and (d), the following parameters which can influence the catalytic activity should be taken into account:

preparation The HFO used in the 50s and 60s was not ordered from a single supplier. Instead it was most likely produced in the lab by a chemical reaction. The procedure was for instance described by Weitzel and Park [39]. After reports that the activity of the HFO varied heavily depending on the batch and details of the preparation, Barrick *et al.* showed that the chemical preparation has to be performed thoroughly since remaining sodium decreases the catalyst's activity [40].

activation Barrick *et al.* also verified that the activity of the catalyst depends on the method of activation [40]. This issue was investigated by Essler as well [36]. While the current supplier recommends to flush the catalyst with dry hydrogen gas while it is heated, the activation was initially performed by heating under vacuum in the earlier studies of the 60s [39, 40]. In the case of Hutchinson and Weitzel *et al.*, detailed information is missing for both data sets.

pressure In principal, the pressure will influence the reaction constant. For instance, Keeler *et al.* have found that the first order rate constant will decrease

with rising pressure for the ortho to para conversion at a temperature of 76 K [26]. However, the pressure differences between both data sets is in this case negligible.

particle size Smaller particles exhibit a larger surface area and will, thus, result in a higher catalytic activity. Keeler *et al.* have summarized the available data for HFO with regard to this topic and found that there is no further increase in activity below a grain size of mesh 50 [26]. This corresponds to the current particle size that is provided by Molecular Products [35]. The experiments whose results are shown in figure 7 were performed with mesh size 20 to 30 by Weitzel *et al.* and mesh size 30 to 50 by Hutchinson.

thermal conditions It was already mentioned that the conversion is highly exothermic for the ortho to para and, thus, highly endothermic for the para to ortho direction. Depending on the thermal conditions, two extremes can be visualized which are either isothermal or adiabatic. Several studies were published for the ortho to para conversion at low temperatures [27]. In this case, isothermal conditions are to be favored. Under adiabatic conditions, the temperature of the catalytic cell will rise. Since the para ortho equilibrium is strongly temperature dependent in this range, the driving force for the reaction will be reduced. Temperature differences between gas inlet and outlet of more than 20 K were reported [27]. While it is clearly stated that Hutchinson *et al.* worked under isothermal conditions, the thermal conditions are not explicitly documented for the particular measurements by Weitzel *et al.* In their publication, Weitzel *et al.* made comparisons between an isothermal setup (HFO mesh size 30 to 50) and an adiabatic one (HFO mesh size 10 to 30). The mesh size given for the additional plot number 9 (which is the one shown in figure 7 (b) of this work) is 20 to 30. One could guess, that this is possibly a typo and that the adiabatic apparatus was used, but this particular grain size is repeated in another plot in this and in two more plots in the almost identical publication [28]. In the NBS report by Weitzel *et al.*, the authors discuss the idea of using the refrigeration generated upon conversion from para to ortho for additional cooling of a liquid hydrogen tank. In more recent works, adiabatic setups are used to study this approach [41, 42].

geometrical dimensions Several authors investigated the influence of the geometrical dimensions of the catalytic cells by varying the outer diameters and lengths as well as the ratio between both (see for instance [26, 43]). For instance, Weitzel *et al.* were able to achieve a more complete conversion from para to ortho when using less catalyst (3 cm^3 compared to 5 cm^3) but in a thinner tube ($\frac{1}{4}$ inch compared to $\frac{3}{8}$ inch) [43]. Their further investigations showed, that it was not the variation in linear velocity, which was assumed to lead to a more efficient diffusion, causing the increased reaction constant. Instead, they, as well as other authors, assumed that the effect was a consequence of different and non-isothermal conditions (see previous bullet point).

The main parameters influencing the catalytic activity were shortly summarized in the previous text. The pressures and space velocities were quite similar for the data sets by Hutchinson and Weitzel *et al.* The smaller particle size of the HFO Hutchinson utilized is actually inconsistent with the lower volumetric reaction constant of his work. However, the preparation and activation of the HFO as well as the thermal conditions also heavily influence the efficiency of conversion. On the one hand, information is partially or fully missing for these aspects. On the other hand, it was shown that it is very likely that corresponding differences exist between both data sets. The author therefore assumes that these are the likely origins of the deviations between both data sets even though a definite explanation cannot be given.

6 Required amount of catalyst

In the following an example calculation will be given of how to estimate the required amount of catalyst for a complete conversion from para to equilibrium or normal hydrogen. It should be pointed out that this can only be a rough estimate. It was shown in section 5.1 that limited and rather poor documented data had to be extrapolated to ambient conditions without explicit experimental verification. This guide recommends to rely on the high temperature data by Weitzel *et al.* for the extrapolation since it covers a wider temperature range. Furthermore, the data is closer to ambient temperature which is primarily discussed in this study.

However, the values by Hutchinson will be also used for validation on the level of uncertainty.

example calculation First, a few parameters have to be fixed. Here, we follow the example of the vaporization test rig where liquid hydrogen is vaporized and shall be catalytically converted at ambient conditions to measure the gas volume flow. In this example, an outlet para concentration of less than 27 % is demanded for a hydrogen mass flow of 4 kg h^{-1} corresponding to 751 standard liter per minute (defined at 273.15 K and 100 kPa). This flow rate is in the order of the maximum hydrogen consumption of a medium sized fuel cell car. Beyond that, the flow rate is relevant for domestic gas metering as well as for certain hydrogen electrolyzers. The specified and deduced parameters are summarized in table 4.

specified parameters		
temperature	T [K]	300
mass flow	m/t [kg h^{-1}]	4
inlet concentration	$\chi_{\text{para,in}}$ [%]	99.8
outlet concentration	$\chi_{\text{para,out}}$ [%]	27.0
deduced parameters		
¹⁾ equilibrium concentration	$\chi_{\text{para,e}}$ [%]	25.08
²⁾ volumetric reaction constant	k_V [$\text{mol cm}^{-3} \text{ s}^{-1}$]	4.74×10^{-5}
molar flow	n/t [mol s^{-1}]	0.551

Table 4: Specified and deduced parameters for the conversion.

¹⁾ equilibrium concentration at this temperature ²⁾ calculated by equation 12 with the parameters for Weitzel *et al.* given in table 3.

Knowing these input values, equation 11 can be rearranged to calculate the required catalyst volume V_{cat} :

$$V_{\text{cat}} = \frac{n}{t} \frac{1}{k_V} \ln \frac{1 - \frac{\chi_{\text{para,in}}}{\chi_{\text{para,e}}}}{1 - \frac{\chi_{\text{para,out}}}{\chi_{\text{para,e}}}} = 42543 \text{ cm}^3 \quad (13)$$

The large volume of more than 42 liters shows that unfortunately HFO seems to be not particularly suitable for a conversion at a temperature of 300 K for this comparably large hydrogen flow.

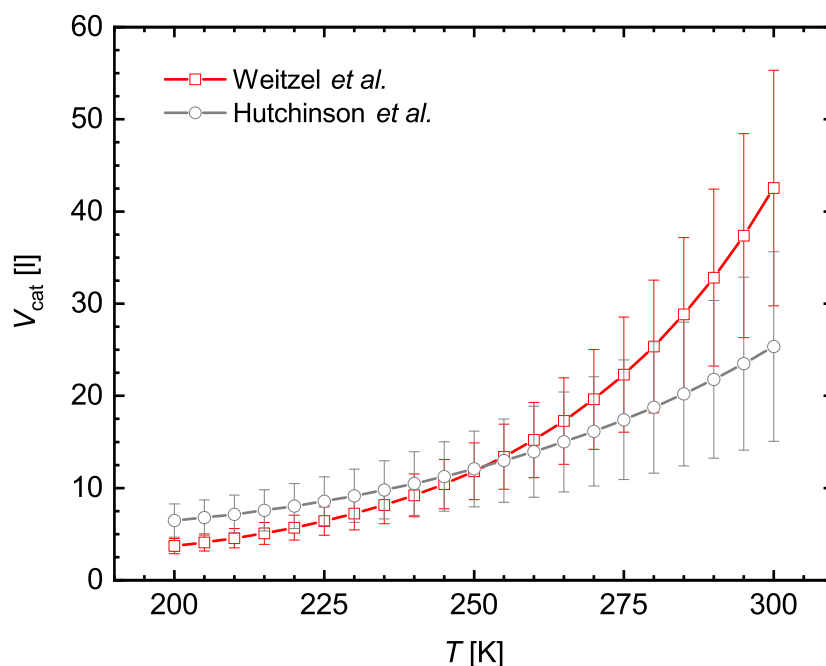


Figure 8: Volume of catalyst V_{cat} required to convert from an inlet para concentration of 99.8% to 27% for a hydrogen mass flow of 4 kg h^{-1} as a function of conversion temperature. The values denoted by the red squares were calculated using the temperature dependence of k_V retrieved from the data by Weitzel *et al.* while for the grey circles the values of Hutchinson *et al.* were used. The uncertainty bars are standard uncertainties that were calculated taking only the uncertainty of the fit coefficients listed in table 3 into account.

Another approach is to reduce the conversion temperature since this increases the volumetric rate reaction constant as shown in figure 7 (d). In figure 8, the red squares denote the required amount of catalyst for the same conditions specified above but as a function of temperature. It can be seen that lowering the temperature from 300 K to 200 K reduces the amount of catalyst by roughly a factor of ten. Unfortunately, the temperature cannot be reduced much further since then the equilibrium concentration of para hydrogen will be too high as shown in figure 2. In addition to the results obtained when utilizing the data by Weitzel *et al.* (red squares), values that were calculated using the extrapolated volumetric reaction rate constants from the data by Hutchinson (grey circles) are shown for compar-

ison. The uncertainty due to the extrapolation is represented for both data sets by the uncertainty bars. These are standard uncertainties that were calculated taking only the uncertainty of the fit coefficients in table 3 into account. The uncertainty increases with temperature and reaches 30 % for Weitzel *et al.* and 40 % for Hutchinson at a temperature of 300 K. Overall, the values obtained by the data from both authors agree on the level of these comparably large standard uncertainties. However, an intersection can be seen at approximately 250 K with the values departing for higher and lower temperatures. This origin of this behavior lies in the qualitatively equal trends of k_V shown in figure 7 (d). To resolve these deviations and reduce the uncertainties of V_{cat} further data for k_V is required.

7 Measurement of the ortho para ratio

It is apparent from the previous sections that it can be difficult to ensure that effluent hydrogen is either still in close to 100 % para configuration or in equilibrium composition. The required amount of catalyst for complete conversion is nothing more than an estimate with large uncertainties. That is why it is recommended to measure the para to ortho hydrogen ratio additionally. Three different techniques that allow to assess the ortho para ratio in a practical manner are presented in the following. A more comprehensive overview is for instance given in the PhD thesis by Essler [17] or the publication by Eisenhut *et al.* [44]. There are obviously other methods to detect the ortho-para ratio which are not further discussed here. Nuclear Magnetic Resonance (NMR) spectroscopy is used in the scientific context but due to the complex and bulky instrumentation not recommended here. Essler used a precise determination of the heat of conversion between the allotropes inside an adiabatic catalytic cell to determine the para ortho ratio in his PhD thesis and corresponding articles [17, 36].

thermal conductivity The large differences in thermal conductivity reported in section 2.2 were already used by Bonhoeffer and Hardeck in 1929 to determine the para to ortho ratio of hydrogen. An electrically heated wire is kept inside an isothermal measuring cell. The resulting temperature of the wire depends on the heat transfer to and, thus, on the thermal conductivity of the gas whereas the

temperature is directly determined from the electrical resistance. Wheatstone bridges, as for instance described and improved by Purcell and Keeler [45] were widely used for this purpose for decades. The cells were further miniaturized. In 2006, Zhou and Sullivan used thin film technology to print a corresponding sensor [46]. Though these systems are popular and partially used until today [41, 42], they have several disadvantages. To obtain a correct measurement, convection needs to be suppressed which is not ideal when monitoring in a dynamic flow system. The method is vulnerable to impurities with a different thermal conductivity like helium. Also, the sensing element is an extremely thin and fragile wire which is likely to mechanically fail. Finally, a calibration of the system with a reference of known ortho para composition is always required. Beyond these general aspects it has to be taken into account that the underlying difference in thermal conductivity has its maximum of over 25 % around 150 K. It drops below 5 % for temperatures of less than 75 K as well as for ambient temperature and above (see figure 3 (a)).

speed of sound A comparably fast option developed at TU Dresden is to measure the speed of sound u . Since this property can be measured with rather low uncertainties, even the small differences in the order of 1 % at ambient conditions are sufficient to determine the ortho para ratio. The method is described in detail by Eisenhut *et al.* in reference [44] whereas a commercially available sensor which directly includes a temperature and pressure measurement was used. Still, to reach lowest uncertainties, a calibration is recommended. Furthermore, a high purity of the gas as well as stable temperature conditions are required.

Raman spectroscopy Another approach that has been brought to an on-line applicable level throughout the recent years and is under further development is the *in-situ* determination of the ortho para ratio by Raman spectroscopy [19, 20, 47–50]. It was shown in section 2 that both spin isomers populate different rotational energy levels. The corresponding transitions can be used to determine the ortho para ratio from the integrated intensity of the corresponding peaks without a need for calibration [48]. Further details on the method and the underlying theory are for instance given in the dissertation by Carl Bunge [47]. Though the Raman signals are inherently weak due the low particle densities in the gas phase, Parrott *et al.* were able to realize an on-line system operating at a temperature of 294 K and a gauge pressure of 0.4 MPa with measuring times of less than one minute [48].

8 Summary, recommendation and outlook

It was shown that para and ortho hydrogen differ in certain thermophysical properties that can heavily influence the measurement of gas flow depending on the method. The equilibrium between both spin isomers is temperature dependent whereas the natural conversion between both states is rather slow. Based on the available literature, the currently available catalyst hydrous ferric oxide was discussed for its potential to ensure conversion from para to equilibrium hydrogen. The required amount of HFO for a particular flow representative of 4 kg h^{-1} is comparably high if the conversion is performed at 300 K and can be reduced by one order of magnitude if the conversion temperature is lowered to 200 K. Unfortunately, this temperature is not easy to realize and maintain. Consequently, HFO can in principle be used to ensure complete conversion from para to equilibrium hydrogen but its use will be accompanied by constructional challenges and probably also financial efforts independently of the used conversion temperature.

That is why it is recommended to use flow measuring methods that are not influenced by the para to ortho ratio. Assuming that the minor differences in density and viscosity reported in section 2.2 have negligible effect on the flow measurement, meter types that due to their measurement principle should be unaffected by the differences in the other physical properties presented in 2.2 are: Coriolis flow meters, differential pressure flow meters, vortex flow meters and mechanical flow meters (like rotary, turbine or diaphragm flow meters). In principle, the discussed ultrasonic flow meters can be used also. Alternatively, due to the slow natural conversion, it can be assumed that hydrogen will remain in the para configuration after vaporization as long as exposition to catalytic materials is minimized, the time scales are short and the densities are comparably low. In case of doubt, estimations of the para concentrations can be performed based on the information provided for the natural conversion in section 3. Furthermore, the para to ortho ratio should be monitored, for which common techniques were introduced.

Possibly, a more suitable catalyst for the para to equilibrium conversion at elevated temperatures is the so called “Apachi” catalyst with the chemical formula

NiO-2.5SiO₂ [38]. Its properties were investigated by Schmauch and Singleton [6]. Unlike HFO, this material is capable of dissociating hydrogen at higher temperatures. This was proven by detection of ortho HD molecules after feeding a catalytic cell with para hydrogen H₂ and para deuterium D₂. Another detailed summary of its properties and also capabilities for the para to ortho conversion can be found in a Final Report to the NASA by T.C. Nast from Palo Alto Research Laboratories [51]. Unfortunately, it was reported in 2019 by Klaus *et al.* that the product which was distributed under the name HSC-197 (Apachi-1) by the company Air Products and Chemicals Inc. is not available anymore [51, 52].

9 Acknowledgement

The author would like to thank the following persons for their help and thorough review of this guide: Christof Gaiser and Bernd Fellmuth from Physikalisch-Technische Bundesanstalt, Carsten Wedler from Imperial College London, Sebastian Eisenhut from Technical University of Dresden, Gregory Aaron Wallace, Jacob Lesauis and Jacob Leachman from the Washington State University and Eric F May from the University of Western Australia. For fruitful discussion and help regarding the flow measurement principles the author also thanks Rainer Kramer, Daniel Schumann and Hans-Benjamin Böckler from Physikalisch-Technische Bundesanstalt as well as Menne Schakel from the Dutch metrology institute VSL. The author also thanks Jürgen Essler for his kind permission to use the microscopic images of HFO. This work was supported through the Joint Research Project “Metrology infrastructure for high-pressure gas and liquified hydrogen flow”. This project 20IND11 MetHyInfra has received funding from the EMPIR programme co-financed by the Participating States and from the European Union’s Horizon 2020 research and innovation programme.

References

- [1] S. Paris and E. Ilisca, *The Journal of Physical Chemistry A* **103**, 4964 (1999).
- [2] P. W. Selwood, in *Advances in Catalysis*, Vol. 27, edited by D. D. Ely, H. Pines, and P. B. Weisz (Elsevier, 1979) pp. 23–57.

- [3] C. F. Ng, *Surface Science* **79**, 470 (1979).
- [4] M. Misono and P. W. Selwood, *Journal of the American Chemical Society* **90**, 2977 (1968).
- [5] E. Justi and G. Vieth, *Zeitschrift für Naturforschung A* **8**, 538 (1953).
- [6] G. E. Schmauch and A. H. Singleton, *Industrial & Engineering Chemistry* **56**, 20 (1964).
- [7] G. E. Kinard, in *Proceedings of the Seventeenth International Cryogenic Engineering Conference*, edited by D. Dew-Hughes, R. G. Scurlock, and J. H. P. Watson (Institute of Physics Publishing, Bristol, 1998) pp. 39–40.
- [8] R. A. Green, R. W. Adams, S. B. Duckett, R. E. Mewis, D. C. Williamson, and G. G. R. Green, *Progress in Nuclear Magnetic Resonance Spectroscopy* **67**, 1 (2012).
- [9] M. J. Assael, J.-A. M. Assael, M. L. Huber, R. A. Perkins, and Y. Takata, *Journal of Physical and Chemical Reference Data* **40**, 033101 (2011).
- [10] J. W. Leachman, R. T. Jacobsen, S. G. Penoncello, and E. W. Lemmon, *Journal of Physical and Chemical Reference Data* **38**, 721 (2009).
- [11] J. B. Mehl, M. L. Huber, and A. H. Harvey, *International Journal of Thermophysics* **31**, 740 (2010).
- [12] S. Z. Al Ghafri, S. Munro, U. Cardella, T. Funke, W. Notardonato, J. P. M. Trusler, J. Leachman, R. Span, S. Kamiya, G. Pearce, A. Swanger, E. D. Rodriguez, P. Bajada, F. Jiao, K. Peng, A. Siahvashi, M. L. Johns, and E. F. May, *Energy & Environmental Science* (2022), 10.1039/D2EE00099G.
- [13] W. G. Fastowski, J. W. Petrowski, and A. E. Rowinski, *Kryotechnik* (Akademie Verlag Berlin, Berlin, 1970).
- [14] R. D. McCarty, J. Hord, and H. M. Roder, *Selected properties of hydrogen (engineering design data): NBS Monograph 186* (National Bureau of Standards, Boulder, 1981).
- [15] G. E. McIntosh, *IOP Conference Series: Materials Science and Engineering* **101**, 012079 (2015).

- [16] K. F. Bonhoeffer and P. Harteck, *Zeitschrift für Physikalische Chemie* **4B**, 113 (1929).
- [17] J. Essler, *Physikalische und technische Aspekte der Ortho-Para-Umwandlung von Wasserstoff*, Phd thesis, Technische Universität Dresden, Dresden (2012).
- [18] Y. Y. Milenko, R. M. Sibileva, and M. A. Strzhemechny, *Journal of Low Temperature Physics* **107**, 77 (1997).
- [19] G. Petitpas, S. M. Aceves, M. J. Matthews, and J. R. Smith, *International Journal of Hydrogen Energy* **39**, 6533 (2014).
- [20] M. J. Matthews, G. Petitpas, and S. M. Aceves, *Applied Physics Letters* **99**, 081906 (2011).
- [21] S. Wagner, *Magma* (New York, N.Y.) **27**, 195 (2014).
- [22] X. Zhang, T. Karman, G. C. Groenenboom, and A. van der Avoird, *Natural Sciences* **1** (2021), 10.1002/ntls.10002.
- [23] A. V. Zhuzhgov, O. P. Krivoruchko, L. A. Isupova, O. N. Mart'yanov, and V. N. Parmon, *Catalysis in Industry* **10**, 9 (2018).
- [24] B. Fellmuth, L. Wolber, Y. Hermier, F. Pavese, P. P. M. Steur, I. Peroni, A. Szymrka-Grzebyk, L. Lipinski, W. L. Tew, T. Nakano, H. Sakurai, O. Tamura, D. Head, K. D. Hill, and A. G. Steele, *Metrologia* **42**, 171 (2005).
- [25] E. Ilisca, *Progress in Surface Science* **41**, 217 (1992).
- [26] R. N. Keeler, D. H. Weitzel, J. H. Blake, and M. Konecnik, in *Advances in Cryogenic Engineering*, edited by K. D. Timmerhaus (Springer US, Boston, MA, 1960) pp. 511–517.
- [27] D. H. Weitzel, C. C. van Valin, and J. W. Draper, *National Bureau of Standards Report* **5515**, 1 (1957).
- [28] D. H. Weitzel, C. C. Valin, and J. W. Draper, in *Advances in Cryogenic Engineering*, *Advances in Cryogenic Engineering*, edited by K. D. Timmerhaus (Springer, Boston, MA, 1960) pp. 73–84.
- [29] H. L. Hutchinson, *A Kinetics Study of the Para-Ortho Shift of Hydrogen*, Masterthesis, University of Colorado, Boulder Colorado (1964).

- [30] H. L. Hutchinson, *Analysis of Catalytic Ortho-Parahydrogen Reaction Mechanisms*, Phd thesis, University of Colorado, Boulder Colorado (1966).
- [31] H. L. Hutchinson, P. L. Barrick, and L. F. Brown, in *Advances in Cryogenic Engineering*, edited by K. D. Timmerhaus (Springer US, Boston, MA, 1965) pp. 190–196.
- [32] H. L. Hutchinson, P. L. Barrick, and L. F. Brown, in *Recent advances in kinetics*, Vol. 63, edited by Thomas E. Corrigan (American Institute of Chemical Engineers, New York, 1967) pp. 18–30.
- [33] H. L. Hutchinson, L. F. Brown, and P. L. Barrick, in *Advances in Cryogenic Engineering*, edited by K. D. Timmerhaus (Springer US, Boston, MA, 1971) pp. 96–103.
- [34] P. J. Donaubaueer, U. Cardella, L. Decker, and H. Klein, *Chemical Engineering & Technology* **42**, 669 (2019).
- [35] Molecular Products Inc., “Ionex®-type o-p catalyst,” https://www.molecularproducts.com/wp-content/uploads/2017/02/OP-Catalyst-166_Rev-D_Technical-Datasheet_OP-Catalyst.pdf (2021), accessed: 2021-08-04.
- [36] J. Essler and C. Haberstroh, in *Advances in Cryogenic Engineering*, AIP Conference Proceedings, edited by J. Weisend and J. Barclay (AIP, 2012) pp. 1865–1872.
- [37] Ø. Wilhelmsen, D. Berstad, A. Aasen, P. Nekså, and G. Skaugen, *International Journal of Hydrogen Energy* **43**, 5033 (2018).
- [38] A. H. Singleton, A. Lapin, and L. A. Wenzel, in *Advances in Cryogenic Engineering*, edited by K. D. Timmerhaus (Springer US, Boston, MA, 1995) pp. 409–427.
- [39] D. H. Weitzel and O. E. Park, *Review of Scientific Instruments* **27**, 57 (1956).
- [40] P. L. Barrick, L. F. Brown, H. L. Hutchinson, and R. L. Cruse, in *Advances in Cryogenic Engineering*, edited by K. D. Timmerhaus (Springer US, Boston, MA, 1965) pp. 181–189.
- [41] Ronald M Bliesner, *Parahydrogen-Orthohydrogen Conversion for boil-off Reduction from Space Stage Fuel Systems*, Masterthesis, Washington State University (2013).

- [42] P. P. Brandt, *Parahydrogen-Orthohydrogen Conversion on Catalyst Loaded SCRIM For Vapor Cooled Shielding of Cryogenic Storage Vessels*, master thesis, Washington State University, Washington (2016).
- [43] D. H. Weitzel, J. H. Blake, and M. Konecnik, in *Advances in Cryogenic Engineering*, edited by K. D. Timmerhaus (Springer US, Boston, MA, 1960) pp. 286–295.
- [44] S. Eisenhut, C. Haberstroh, M. Klaus, and A. Schwab, in *46th Annual Meeting of the Deutscher Kaelte und Klimatechnischer Verein 2020*, edited by Deutscher Kaelte und Klimatechnischer Verein (Curran Associates, Inc., 2020 Online) p. AA I 17.
- [45] J. R. Purcell and R. N. Keeler, *Review of Scientific Instruments* **31**, 304 (1960).
- [46] D. Zhou and N. S. Sullivan, in *AIP Conference Proceedings* (AIP, 2006) pp. 1687–1688.
- [47] C. D. Bunge, *A High-Fidelity, Continuous Ortho-Parahydrogen Measurement and Conversion System*, Phd thesis, Washington State University, Pullman (2021).
- [48] A. J. Parrott, P. Dallin, J. Andrews, P. M. Richardson, O. Semenova, M. E. Halse, S. B. Duckett, and A. Nordon, *Applied Spectroscopy* **73**, 88 (2019).
- [49] R. C. Gillis, T. Bailey, F. X. Gallmeier, M. A. Hartl, and E. B. Iverson, *Journal of Physics: Conference Series* **1021**, 012062 (2018).
- [50] L.-M. Sutherland, J. N. Knudson, M. Mocko, and R. M. Renneke, *Nuclear Instruments and Methods in Physics Research Section A: Accelerators, Spectrometers, Detectors and Associated Equipment* **810**, 182 (2016).
- [51] T.C. Nast, "Investigation of para-ortho hydrogen reactor for application to spacecraft sensor cooling," <https://ntrs.nasa.gov/citations/19840007889> (1983), tech. Rep. LMSC-D877499 (Palo Alto, California).
- [52] M. Klaus, A. Schwab, C. Haberstroh, K. Eckhardt, Y. Beßler, J. Baggemann, and T. Cronert, *IOP Conference Series: Materials Science and Engineering* **502**, 012161 (2019).



Bundesministerium
für Wirtschaft
und Klimaschutz

Die Physikalisch-Technische Bundesanstalt, das nationale Metrologieinstitut, ist eine wissenschaftlich-technische Bundesoberbehörde im Geschäftsbereich des Bundesministeriums für Wirtschaft und Klimaschutz.



Physikalisch-Technische Bundesanstalt
Nationales Metrologieinstitut
ISNI: 0000 0001 2186 1887

Bundesallee 100
38116 Braunschweig

Presse- und Öffentlichkeitsarbeit

Telefon: (0531) 592-93 21
Fax: (0531) 592-30 08
E-Mail: presse@ptb.de
www.ptb.de